A Photographic Apparatus for Angular-Distribution Measurements

SYLVAN RUBIN
W. K. Kellogg Radiation Laboratory, California Institute of Technology, Pasadena, California
(Received September 12, 1947)

A scattering camera was designed and constructed to measure the angular distribution of heavy charged particles emitted from nuclear reactions by means of the tracks which they produce in a photographic emulsion. It uses a single 2-in×4-in. plate to detect particles emitted in the angular range of 25° to 160° to the direction of the incident beam of bombarding particles. The camera has been used to investigate the angular distribution of the alpha-particles from the reaction $Li^7(p, \alpha)\alpha$, the long-range alpha-particles from $F^{19}(p, \alpha)O^{16}$, and the resonance scattering of protons in $Be^9(p, \gamma)B^{10}$. These reactions have been investigated over bombarding proton energies covering the range of interest in each reaction. This apparatus has been found to be effective for detailed measurements of angular distributions, with very high resolution of energy and of angle, even for reactions with very low yield, using thin solid targets. Fogging of the plates by soft x-rays from the target has been reduced by suitable target supports. Some results and conclusions concerning the above reactions are reported.

I. INTRODUCTION

THE determination of the angular distribution in the yield of nuclear reactions provides information on the characteristics of the quantum states involved in the reactions. The assignment of appropriate quantum numbers to various excitation levels in light nuclei is facilitated by a knowledge of the angular distribution in reactions involving those levels. The theory of the calculation of the angular distribution of resonance reactions is treated in several papers.[1–4]

Most of the experimental work on angular distributions between 1933 and 1940 was done with thick targets,[5–13] so that not much is known from these experiments of the variation of angular distribution with energy, except for Neuert's work.[14] Since 1940 several precision experiments have been done, giving detailed measurements of the angular distributions in a few light element reactions.

The reaction $H^2(d, p)H^3$ has been investigated up to 400 kev,[15,16] and the angular distribution is given by the function: $1+A\cos^2\theta$, where A increases smoothly to a value of 1.5 at 400 kev.

$H^2(d, n)He^3$ has been done from 500 kev to 1.8 Mev,[17] and the angular distribution is again given by $1+A\cos^2\theta$, with the curve for A *vs.* energy fitting smoothly to that for the protons from $H^2(d, p)H^3$, going to about 3.3 at 1.8 Mev.

$Li^7(p, \alpha)\alpha$ has been investigated up to 1.4 Mev.[18–20] It also fits the distribution function, $1+A\cos^2\theta$, at all energies; however A reaches a maximum of 2.1 at about 800 kev, and then slowly decreases.

$F^{19}(p, \alpha)O^{16}$ has been studied by several investigators,[21,22] and has been shown to have very complex distributions which change rapidly with energy. Results on this reaction are still very incomplete, because of the low yield of the long-

[1] E. Gerjuoy, Phys. Rev. **58**, 503 (1940).
[2] C. L. Critchfield and E. Teller, Phys. Rev. **60**, 10 (1941).
[3] E. Eisner, Phys. Rev. **65**, 85 (1944).
[4] G. Breit and B. T. Darling, Phys. Rev. **71**, 402 (1947).
[5] F. Kirchner, Physik. Zeits. **34**, 777 (1933).
[6] J. Giarratana and C. G. Brennecke, Phys. Rev. **49**, 35 (1936).
[7] A. E. Kempton, B. C. Browne, and R. Maasdorp, Proc. Roy. Soc. **157**, 386 (1936).
[8] H. Neuert, Physik. Zeits. **38**, 122 (1937).
[9] H. Neuert, Physik. Zeits. **38**, 618 (1937).
[10] H. Neuert, Zeits. f. tech. Physik **19**, 576 (1938).
[11] R. O. Haxby, J. S. Allen, and J. H. Williams, Phys. Rev. **53**, A921 (1938).
[12] A. Ellett and R. D. Huntoon, Phys. Rev. **54**, A87 (1938).
[13] R. O. Haxby, J. S. Allen, and J. H. Williams, Phys. Rev. **55**, 140 (1939).
[14] H. Neuert, Ann. d. Physik **36**, 437 (1939).
[15] R. D. Huntoon, A. Ellett, D. S. Bayley, and J. A. Van Allen, Phys. Rev. **58**, 97 (1940).
[16] H. P. Manning, R. D. Huntoon, F. E. Myers, and V. J. Young, Phys. Rev. **61**, 371 (1942).
[17] W. E. Bennett, C. E. Mandeville, and H. T. Richards, Phys. Rev. **69**, 418 (1946).
[18] V. J. Young, A. Ellett, and G. J. Plain, Phys. Rev. **58**, 498 (1940).
[19] C. D. Swartz, H. H. Rossi, B. Jennings, and D. R. Inglis, Phys. Rev. **65**, 80 (1944).
[20] S. Rubin, W. A. Fowler, and C. C. Lauritsen, Phys. Rev. **71**, 212 (1947).
[21] W. B. McLean, A. Ellett, and J. A. Jacobs, Phys. Rev. **58**, 500 (1940).
[22] H. H. Rossi and C. D. Swartz, Phys. Rev. **65**, 83 (1944).

range alphas, and the consequent difficulty of obtaining detailed data.

This paper describes a photographic technique for measurement of the angular distributions of some nuclear reactions. It has been used up to the present on the $Li^7(p, \alpha)\alpha$, and $F^{19}(p, \alpha)O^{16}$ reactions; and on the scattering of protons from beryllium.

II. APPARATUS

This "scattering camera" is partly based on the design published by Chadwick, May, Pickavance, and Powell,[23] which was a single-plate scattering camera for use in measuring the angular distribution of scattering of high energy particles from a cyclotron on a gas target. Its chief feature was the use of a single plate, so as to take advantage of the property of an emulsion of not only integrating the yield of heavy ionizing particles, but of defining their position of impact with the emulsion, and therefore their direction of travel from a sufficiently small source. This feature greatly increases the efficiency of a photographic plate over ionization chambers for a given angular resolution. Because both the solid angle subtended by the target at the chamber aperture, and that subtended by the chamber aperture at the target must be small, the yield will be inversely proportional to the square of the angular resolution for ionization chambers, or counters; whereas it is inversely proportional to the first power of the resolution for photographic plates used in this way, since there is no restriction on the solid angle subtended by the plate at the target.

The camera which has been constructed uses a single plate in a manner similar to that described by Chadwick, *et al.* However, to obtain still greater efficiency in detection it was decided to design it to use solid targets for either disintegration or scattering experiments, rather than the "tubular" gas target, in which energy loss in the consecutive axial elements contributing to the yield at each corresponding angle is accumulative. In a thin solid target there is only one element supplying particles at all angles and thus much less energy loss for a given yield, or conversely, more yield for a given energy resolution and angular resolution (Fig. 1).

For ease of construction the camera is a shallow cylindrical tank, about 6 in. in diameter and $1\frac{1}{2}$ in. deep, made of $\frac{1}{8}$-in. wall brass pump liner, with $\frac{3}{8}$-in. thick brass covers in which rubber gaskets are recessed. Six bolts, spaced uniformly around the exterior, clamp the two covers together to make the tank vacuum tight. The axis of the target-mounting assembly and collimating tube is 1 in. off-center, as indicated in the drawing, in order to allow sufficient space at one side for the plateholder. Two brass blocks, after being brazed to the exterior of the cylinder, were coaxially bored on a milling machine, and close-fitting circular flanges were soldered into these blocks so as to maintain accurate alignment. A reamed hole through each of these blocks for two of the six cover-clamping bolts positively aligns the covers with respect to this axis. The camera is mounted on the end of the beam analyzer of the electrostatic accelerator by means of the front flange, which also holds a tubular Lucite window and the tube containing the beam-defining aperture and shielding-baffle aperture. On the rear flange is mounted the target assembly and shield tube. The joints between all external components were sealed with rubber gaskets.

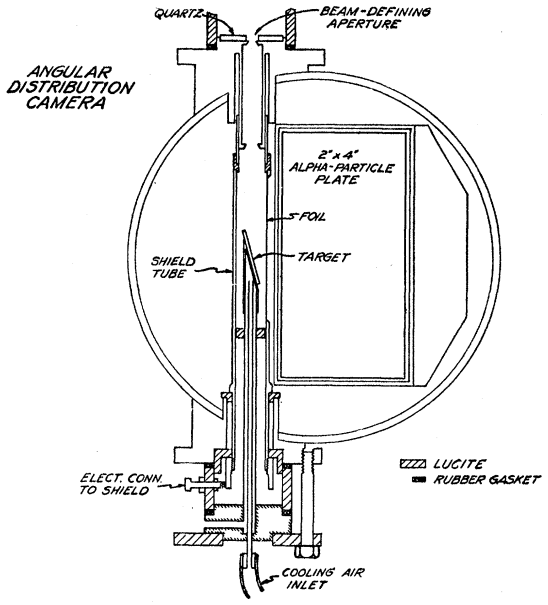

FIG. 1. Schematic drawing of scattering camera. One of several modifications.

[23] J. Chadwick, A. N. May, T. G. Pickavance, and C. F. Powell, Proc. Roy. Soc. **183**, 1 (1944).

The target is located at the central plane of the camera, on the off-center axis of the flanges. The various targets used have been mounted obliquely at 20°–25° to the incident beam, on a tubular thimble which slips on the end of a target-support tube. This tube is soldered to a brass disk which is separated from the rear flange by Lucite insulators to make possible measurements of the ion current to the target. For the work in which thin foil targets were used, the target mounting was modified to include a quartz window cemented in the rear disk, so that the ion beam, after penetrating the foil target, could be observed by the fluorescence it produced on the window. This was extremely useful in accurately aligning the beam in the camera. The target support tube is coaxial with a $\frac{1}{2}$-in. diameter shield tube which completely encloses it, and which is also insulated, so as to be part of a Faraday cage arrangement in which a negative potential of 90 volts on the shield relative to the target prevents loss of electrons from the target under ion bombardment. Into the front flange is screwed the aperture tube, with an insulated tip where it joins the shield tube mounted on the rear flange. The aperture tube carries a quartz disk with a small hole in its center for locating the ion beam, the beam defining aperture just below the quartz, and about $2\frac{1}{2}$ in. farther down a larger aperture to prevent ions scattered by the edges of the defining aperture from striking the electrostatic shield. The defining aperture is usually a $\frac{3}{32}$-in. circular, thin-edged hole, but can be stopped down to $\frac{1}{32}$ in. by an insert.

Cut in the wall of the shield tube is a rectangular slot, $1\frac{3}{4}$ in.$\times\frac{1}{4}$ in., in which is mounted an aluminum window frame. The frame is shaped to support a curved thin aluminum-foil window $\frac{3}{16}$ in. wide and $\frac{7}{8}$ in. long, of $\frac{5}{8}$-in. radius of curvature, in a position $\frac{5}{16}$ in. from the center of the target. Various foil thicknesses are used to stop the scattered particles from the incident beam, but to allow the reaction products of longer range to penetrate to the photographic plate.

The aluminum-foil window used for the earlier data on $Li^7(p, \alpha)\alpha$ was a straight, rather than curved, foil. However, the shortening of the tracks in the backward direction caused by the decrease of energy in the laboratory system, combined with the increased absorption of the straight foil at large angles from the normal, gave such short tracks at large backward angles that it was difficult to measure track density in this region. Use of a curved window after the first 4 plates was a considerable improvement, although there was not sufficient space available to make its radius equal to its distance from the target. Also, by using a set of removable aluminum window frames the window thickness could be changed more conveniently.

The photographic plates which have been used are 2-in.$\times$4-in. Eastman fine-grain alpha-particle plates with an emulsion about 20–25 microns thick. The plates were obtained about 2 dozen at a time, and successive batches were progressively better, giving closer grain spacing and clearer tracks. In the last emulsions used the mean-grain spacing is less than 1μ. All plates were on 0.043-in. glass, so as to be suitable for dark-field illumination with standard slide-illuminating condensers. One plate is used for each run, being mounted emulsion-side up in a plate holder fastened to one cover of the camera such that the long edge of the plate is parallel to the incident beam, which is 15 mm above the plane of the emulsion. Particles from the target, after penetrating the aluminum-foil window, thus strike the emulsion at a small angle to its plane along a circular arc on the emulsion at a constant distance of 50 mm from the target. From any point along this arc, between 25° and 155° to the direction of the incident beam, the entire effective target is visible through the aluminum window. The plate holder is closed by a light-tight hinged shutter which is operated from outside the camera with a lever mounted in a rubber diaphragm.

The most recent emulsions, which produce the best tracks, have such a low proportion of gelatine that there is frequent peeling of parts of the emulsion when the plate is put in a vacuum. This occurs along the edges of the plates, and sometimes quite a large piece of emulsion curls up or breaks off. To prevent these loose edges from projecting into the path of the particles to be detected a clip was made of 0.006-in. shim steel, to fit snugly on the front edge of the plate. The clip extends almost to the arc along which observations are to be made, and ensures that the

path to that arc from the target does not become obstructed by loose emulsion. Occasionally the peeling caused the loss of some data at the smallest or largest usable angles, in which cases the run was repeated.*

III. TARGETS

In preliminary tests, with various types of lithium and fluorine targets under proton bombardment, considerable trouble was encountered with fogging of plates, even after the target had been completely enclosed to prevent escape of any scattered protons. It was soon found that this was caused by soft x-rays from the target, as it could be eliminated by using only light elements in compounds with lithium or fluorine, and for the backing of thin targets. Thin targets of LiOH on steel or on aluminum gave excessive x-rays but were satisfactory on a beryllium backing. A thick CaF_2 target gave considerably more fog than a thick BeF_2 target. This variation in the action of various target-backing materials corresponds to the rapid increase in x-ray yield with atomic number.[24]

A run made with 700-kev protons bombarding a clean, thick, beryllium-metal target showed no significant yield of particles through an aluminum window of 3.93-mg/cm^2 surface density, so that beryllium provides a satisfactory backing for thin targets for proton bombardment, and was used for all the work described in this paper. This result is in agreement with the known ranges of the heavy particles from the disintegration of beryllium by protons.

The preliminary work on $F^{19}(p, \alpha)O^{16}$ was done with a thin BeF_2 target made by placing a drop of HF diluted with alcohol on the surface of a beryllium plate for a few seconds, then washing the excess off with alcohol. However, because of the very low cross section for long-range alphas, even this target gave excessive x-ray fogging. Although tracks were visible in it, they were difficult to count. Some targets were then made by mounting 0.5-micron thick beryllium foils on an oblique target thimble, with no backing behind the foil. The foils were coated with BeF_2 by holding a small drop of HF close to the foil for a short time. These made excellent thin targets, although fragile, requiring frequent replacement. Very satisfactory plates were obtained with no visible fog and easily observed tracks, in spite of the very low yield per proton.

IV. ASSOCIATED APPARATUS

The camera is mounted on the end of the ion-beam analyzer of the electrostatic generator which can, under present operating conditions, go to a voltage of 1.4 Mv. For the $Li^7(p, \alpha)\alpha$ experiments and the preliminary work on $F^{19}(p, \alpha)O^{16}$, a simple magnetic analyzer was used; for later work a combination electrostatic and magnetic analyzer was available. These analyzers, combined with an automatic electronic voltage-regulator operated by pick-up electrodes at the end of the analyzer, hold the voltage to within less than 1-kev variation, and hold the ion beam very steady in position.

The ion energy is determined by the output of a rotating sector generating voltmeter mounted in the top of the generator tank. This is calibrated with the narrow gamma-ray resonances of $F^{19}(p; \alpha, \gamma)O^{16}$ and $Be^9(p, \gamma)B^{10}$. In addition, since the advent of the electrostatic analyzer the analyzer deflection voltage has been found to be very convenient for ion-energy determination, and is also calibrated in terms of these γ-ray resonances.

The target assembly, electrically insulated by Lucite bushings, is connected to a low leakage 1 μf condenser, the voltage of which is measured by a quartz-fiber electrometer to give the integrated ion charge to the target. A galvanometer from the condenser to ground gives continuous readings of the instantaneous ion current.

V. MEASUREMENTS

The plates are measured on a microscope fitted with a mechanical stage driven by a micrometer screw and a paraboloidal dark-field illuminating condenser. Most of the observations are made with 8-power or 40-power objectives, depending on the track density, and a 25-power hyperplane eyepiece fitted with a counting reticle, dividing the circular field of view into about 16 squares (cut off a little at the corners).

* Note added in proof: The latest shipment of plates does not peel.

[24] M. S. Livingston, F. Genevese, and E. J. Konopinski, Phys. Rev. **51**, 835 (1937).

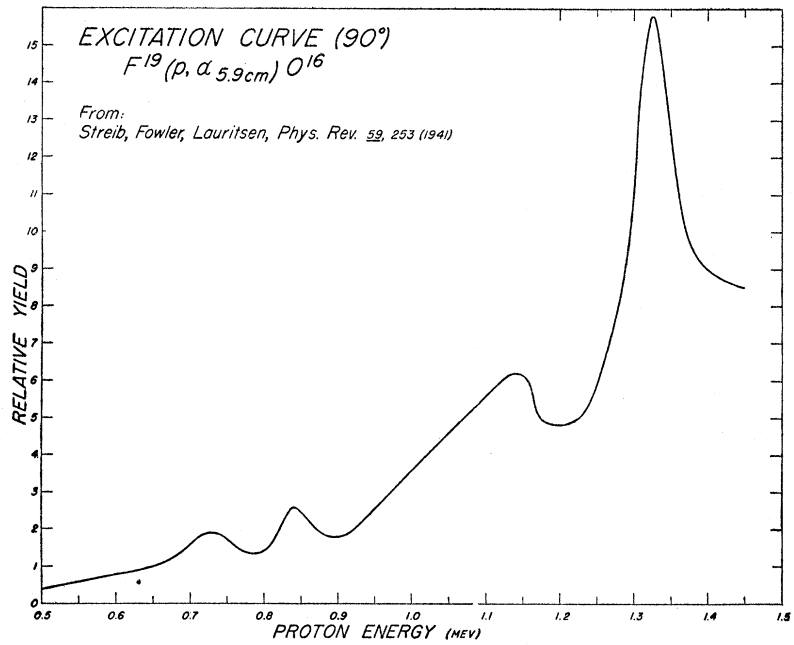

FIG. 2. Excitation curve for emission of long-range alpha-particles from proton bombardment of fluorine.

Before the plate can be measured it is necessary to lay out a coordinate system. The plate is examined under the microscope at several positions and adjusted each time so that the average direction of the tracks is parallel with the horizontal reticle lines, and a line is scribed on the plate through that point, also parallel with the reticle. This can be done to an accuracy of about 1° when the tracks are of reasonable length. The plate is then clamped on a coordinate-layout block which has lines scribed at 5° intervals radiating from a punch mark. The plate is adjusted so that the convergence point (actually a small area) of the lines previously scribed on the plate is centered on the punch mark, and the long edge is normal to the 90° line. This convergence point is about $\frac{1}{2}$ in. off the plate, and the adjustment is made by checking with a straightedge. Two arcs are scribed on the emulsion, at 45.7- and 49.7-mm radius about the punch mark, with a sharp pair of dividers. Since the center of the target is 15 mm above the plane of the emulsion, the center of this 4-mm wide arc is at 50 mm from the target. Radial lines are drawn on the emulsion directly above the standard lines on the layout block. The plate is then ready for counting tracks.

It is clamped on the microscope stage, adjusted so that a radial line is parallel to the micrometer motion of the stage and passes through the center of the field of view. Starting near one edge of the 4-mm wide arc, all tracks are counted within a rectangular swath of a little less than 4 mm in length and some convenient width, depending on the track density. Various combinations of 8x and 40x objective, and 1-, 2-, or 4-squares width are used. The ratios of these widths, in actual distance, are known to about 3 percent by direct calibration measurements on a glass-reticle scale which had previously been measured on a comparator microscope. These calibration measurements were made with all available combinations of eyepieces and objectives.

The solid angle from the target is determined from the swath dimensions and the angle of incidence of the particles on the emulsion. For most counting, when the track density is most convenient, the 8x objective is used, and a swath 1 sq. wide (0.213 mm) and 0.140 in. long is counted. This, after correcting for the oblique incidence, is a solid angle from the target of 9.2×10^{-5} steradian, or 7.3×10^{-6} of a sphere. It is not difficult to count up to 1500 tracks in this area with this magnification, or several times more, using higher magnification. However, it is more convenient to use the lower magnification, thus setting an upper limit of about 2×10^{8} emitted particles (assuming isotropic distribution) for

each run. Even with thin targets this is usually obtained with a few hundred microcoulombs of bombarding particles.

After the counting is done at a sufficient number of different angles on the plate, depending on the detail and accuracy desired, the data is then corrected.

VI. CORRECTIONS

Three corrections are required for this method of obtaining angular distributions. First the angles measured in the plane of the plate must be converted to angles in a plane including the incident beam and the point where the tracks are observed. Since all measurements are made on an arc at 50 mm from the target, and the distance between the target and the plane of the plate is constant, this correction was computed only once and tabulated in the form of the cotangent of the corrected angle in terms of the observed angle. The formula used for this correction is

$$\sin\theta=\frac{\left(\sin^2\varphi+\left(\frac{h}{r}\right)^2\right)^{\frac{1}{2}}}{\left(1+\left(\frac{h}{r}\right)^2\right)^{\frac{1}{2}}},$$

where θ is the angle with respect to the incident beam, φ is the angle in the plane of the plate (observed), h is the normal distance from the target to the plate, and r is the radius from the target to the point of measurement.

The other two corrections are for conversion of the data in laboratory coordinates to center-of-mass coordinates, involving correcting both the angular coordinate and the yield per unit solid angle.

The correction to the angular coordinate is given by the exact expression:

$$\operatorname{ctn}\theta=\operatorname{ctn}\theta_c+\alpha\csc\theta_c,$$

where θ is the angle in laboratory coordinates, θ_c is the angle in C.M. coordinates, and

$$\alpha=\left[\frac{M_1M_2E_1}{MM_3Q+M_0M_3E_1}\right]^{\frac{1}{2}},$$

where M_0 is the mass of the stationary target nucleus, M_1 is the mass of the incident nucleus, M_2 is the mass of the observed nucleus, M_3 is the mass of the residual nucleus, $M=M_0+M_1=M_2+M_3$, E_1 is the energy of the incident nucleus, in laboratory coordinates, and Q is the reaction energy.

A convenient approximation, which is sufficiently accurate for this work, is

$$\operatorname{ctn}\theta_c=\operatorname{ctn}\theta-\alpha\csc\theta.$$

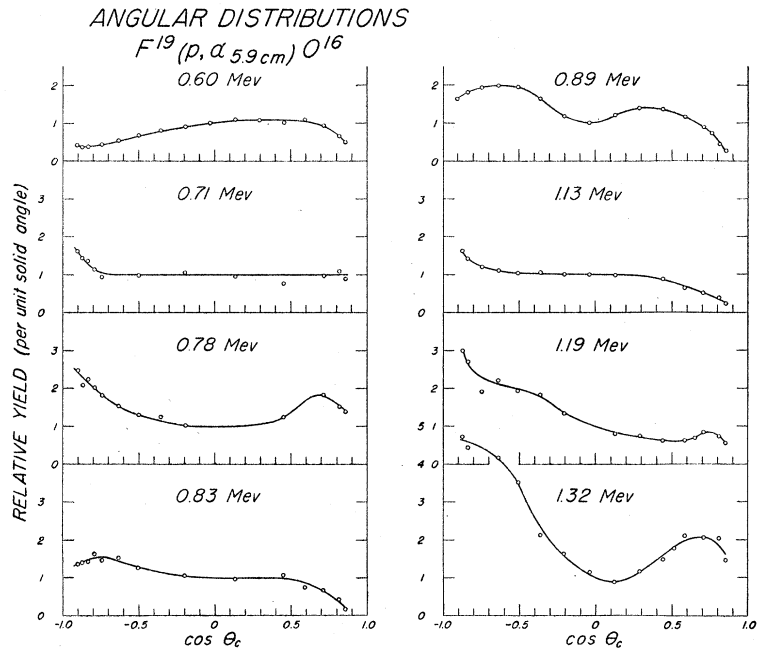

FIG. 3. Preliminary angular-distribution curves of long-range alphas from protons on fluorine. Yield coordinate normalized to unity at 90°.

Since the solid angles in which counts are made are very small in angular extent, the differential expression for the ratio of the solid angle in the C.M. system to that in the laboratory system is sufficiently accurate. It is

$$\frac{d\Omega_c}{d\Omega}=\frac{\sin\theta_c\ d\theta_c}{\sin\theta\ d\theta}=\frac{(1+2\alpha\cos\theta_c+\alpha^2)^{\frac{3}{2}}}{1+\alpha\cos\theta_c}\simeq 1+2\alpha\cos\theta_c.$$

If N is the number of tracks in equal solid angles in the laboratory system and N_c the number in equal solid angles in the C.M. system, then

$$N_c=N\left(\frac{d\Omega}{d\Omega_c}\right)\simeq N(1-2\alpha\cos\theta_c).$$

The use of the first approximation to the correction is sufficiently accurate, since the maximum value of α in any of this work was 0.11 for proton scattering on Be^9. In this case the error in neglecting higher terms is about 2 percent at extreme angles. This is small compared to the statistical uncertainty in the number of tracks at each angle.

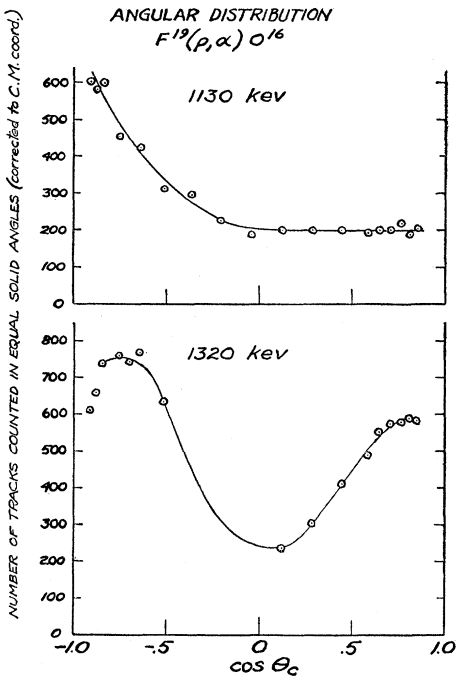

FIG. 4. Angular distribution curves of long-range alphas. Relative bombardment adjusted to give same 90° yield. The yield coordinate is approximately equal to actual tracks counted, so that statistical uncertainty can be estimated.

VII. RESULTS

I. $Li^7(p, \alpha)\alpha$ reaction

The results of the work on the angular distribution of the alpha-particles emitted in this reaction over a range of proton energies of 400 to 1400 kev have been previously published.[20]

II. $F^{19}(p, \alpha)O^{16}$ reaction

Another problem investigated was the reaction $F^{19}(p, \alpha)O^{16}$, leading to the emission of 5.9-cm alphas and O^{16} in its ground state. Because of the resonance character of this reaction in the energy range of 600- to 1400-kev proton energy, it was desired to investigate the angular distribution of the alphas at the various resonances, shown in Fig. 2.[25] For this purpose it was necessary to use a sufficiently thin target to obtain adequate resolution. This reaction proved to be considerably more difficult to work with than the $Li^7(p, \alpha)\alpha$ reaction, because of the low yield. It was necessary to make considerably heavier bombardments to obtain a sufficient yield of the alpha-particles, and, as a result, the plates became somewhat fogged by the x-rays from the thick beryllium-target backing. However, a preliminary set of curves was obtained, although the fogging of the plates limited the extent and accuracy of the track counting. They show a considerable variation of the character of the angular distribution from one resonance to another, as is shown in Fig. 3, but the accuracy is insufficient for analysis of the angular distributions into cosine powers.

Some plates were obtained later, using a different type of target. A thin foil of beryllium metal about 0.5μ thick, prepared by evaporation,[26] was mounted on the target support and coated with a thin film of BeF_2 by holding it in HF vapor for a short time. This target produced negligible x-ray intensity, so that the plates were free from x-ray fog. The track counting was much easier and more reliable, and more tracks were counted than on the earlier plates. However, these plates were not satisfactory because of a faulty window. The problem of separating the alphas and the scattered protons, especially above 1 Mev where

[25] J. F. Streib, W. A. Fowler, and C. C. Lauritsen, Phys. Rev. **59**, 253 (1941).

[26] The beryllium foils were made by Dr. H. Bradner, Radiation Laboratory, Berkeley, California.

the alphas do not have very much more range than the protons, also contributed to the difficulty of working with this reaction, since the residual range of the alphas was very short after penetrating the foil which stopped the protons.

After a new window was prepared two plates, at 1140 kev and at 1330 kev, were obtained. These angular distributions are shown in Fig. 4. It will be noted that they essentially agree with the preliminary distributions in indicating a very complex variation of yield with angle.

The asymmetric character of these angular distributions indicates that interference effects in the wave function of the emitted alphas are being produced by adjacent or overlapping levels in the compound Ne^{20} nucleus, as odd powers of $\cos\theta$ in the angular distribution function can arise only from interference terms in the wave function. Also, the shapes of the distributions at small angles to the beam, where the effect of high powers of $\cos\theta$ will be significant, are such that terms of higher power than $\cos^2\theta$ appear to be needed to fit the data. If terms up to $\cos^3\theta$ or $\cos^4\theta$ are needed, this indicates an appreciable effect from d-wave incident protons.

At low energy the shift toward higher yield in the forward direction, instead of backward, as observed at higher energies, tends to agree with McLean, Ellett, and Jacobs'[21] result at 400 kev.

The angular distributions at 1140 and 1330 kev are satisfactorily fitted by the expressions—

$$1140 \text{ kev: } 1-\tfrac{1}{3}\cos\theta+\cos^2\theta-\cos^3\theta;$$
$$1330 \text{ kev: } 1-\cos\theta+6\cos^2\theta+\cos^3\theta-5\cos^4\theta.$$

The even powers of $\cos\theta$ at the prominent resonance at 1330 kev may be compared with the theoretical angular distribution from an assumed $^2P_{\frac{1}{2}}$ (even parity) ground state of F^{19}, reacting with d-wave protons to produce a compound level of $J=2$, which can decay to He^4 and the ground state of O^{16}. This is $\cos^2\theta-\cos^4\theta$, which is in fair agreement with the observed distribution at this resonance, if it be assumed that the constant term represents background caused by adjacent levels, and the odd powers of $\cos\theta$ are due to interference between the resonance and the background wave functions.[27]

[27] The fitting of the cosine power functions, and the calculation of the theoretical angular distributions were done by Professor R. F. Christy in the course of analyzing the data presented in this paper.

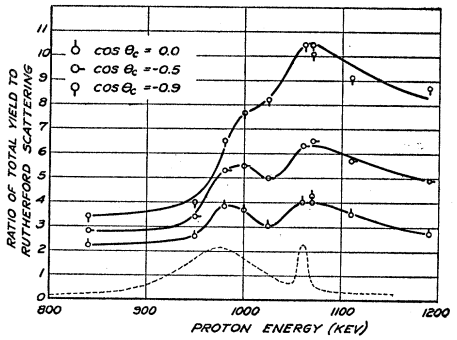

FIG. 5. Excitation curves of resonance scattering of protons from beryllium. Dotted curve is γ-ray yield from beryllium target of the same thickness.

The weaker resonance at 1140 kev shows a larger interference effect, so that an estimate of the character of this level is less clear.

Some penetration factors recently calculated by R. F. Christy show that the apparent yield from d-wave protons in this reaction is not unreasonable.

III. $Be^9(p, p)$ scattering

It was thought that an investigation of the angular distribution of the protons scattered from Be^9 at the γ-ray resonance energies in the reaction $Be^9(p, \gamma)B^{10}$ would give some information on the reason for the difference in the character of the two prominent γ-ray resonances at 972 and 1060 kev, shown in the dotted curve of Fig. 5.[28] The 972-kev resonance is a broad one and the 1060-kev resonance is very narrow, suggesting that the broad one may be due to s- or p-wave protons, and the narrow resonance to higher orbital momentum. A difference in orbital momentum might be expected to show up in the angular distribution of the resonance-scattered protons at the two energies.

The chief difficulty in observing the resonance scattering is that it is combined with Coulomb scattering, and these cannot easily be considered separately because of interference effects, especially at the angles where they are of equal magnitude. Furthermore, the reaction $Be^9(p, d)Be^8$ gives deuterons of approximately the same range as the elastically scattered protons, and the reaction $Be^9(p, \alpha)Li^6$ yields alphas of about half their

[28] C. C. Lauritsen, T. Lauritsen, and W. A. Fowler, Phys. Rev. **71**, A279 (1947).

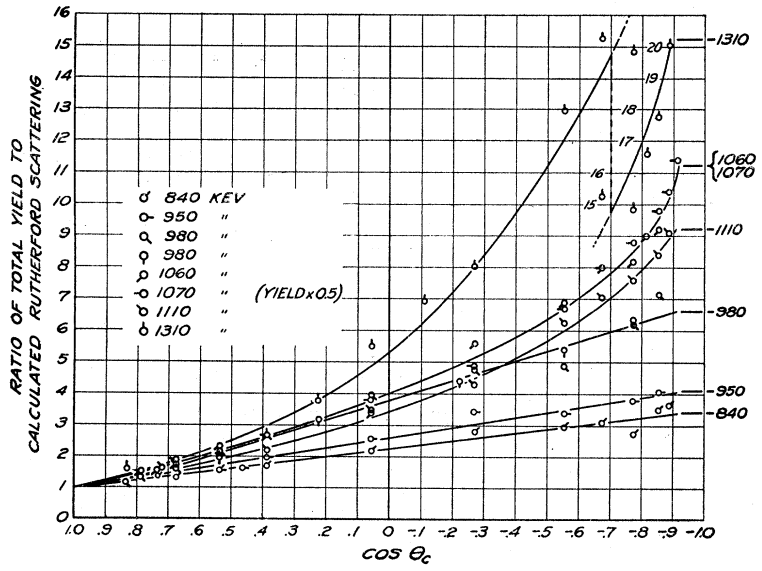

FIG. 6. Ratio of total yield of emitted particles to Rutherford scattering for various energies of protons bombarding beryllium.

range. All the emitted particles were included in the counting, since the deuteron tracks could not, in any case, be distinguished from the proton tracks, and the alpha-tracks were not easily recognizable. The very short ranges of all the particles meant that there were only about 10 grains per proton track, so that statistical fluctuations would make it difficult to distinguish them from the shorter, but more heavily ionizing, alpha-tracks.

A beryllium foil, 0.23 microns thick, was used for the scattering target. It was mounted on a 0.001-in. thick copper-foil washer, with a $\frac{5}{32}$-in. diameter aperture, set at 110° to the beam. The supporting thimble was cut out on one side below the target-supporting washer, so that particles observed at angles smaller than 110° came from the back of the target, and those observed at larger angles came from the front. No stopping window was used, as the particle ranges were already so short that it would have been useless to try to stop the alphas, as the remaining proton range would then be so short as to make the observations impossible.

Since the cross section for scattering is very large, an adequate yield of tracks is obtained, even from a very thin target, with a very small bombarding charge. To reduce the target current and improve the geometry a defining aperture of $\frac{1}{32}$-in. diameter was used, with a protective baffle of $\frac{1}{16}$-in. diameter, so that it was impossible for the beam to strike the copper-support foil. A smaller condenser (0.1 μf) was used in the current-integrating circuit. After some preliminary runs to determine the optimum bombarding charge, it was found that 1.20 microcoulombs of protons on the 0.23-micron foil was convenient.

Because of the shortness of the tracks a high magnification was more satisfactory for seeing them easily, using a 40-power objective and the 25-power eyepiece with the counting reticle. At this magnification it was possible to count track densities as high as 20,000 tracks per sq. mm before they became too numerous to easily distinguish individual tracks. The exposure of the plates was adjusted to make the track density approximately 20,000 per sq. mm at 25°, so that the much smaller yield at large angles would be sufficient to obtain good statistics. The results given below are based on measurements of 10 plates,[29] taken at various energies in the neighborhood of the γ-ray resonances.

The Rutherford scattering of protons on Be^9 per unit solid angle is given by

$$n(\theta)=1.04\frac{n_0N}{\beta}\left(\frac{10r_0}{9E}\right)^2,$$

where n_0 is the number of incident protons, N is the number of Be atoms/cm², $\beta=(1-\cos\theta)^2$

[29] Three of these plates were measured by G. S. Kenny, who is carrying out further development of this method.

$=4\sin^4(\theta/2)$, $r_0=2.82\times10^{-13}$ cm, and $E=$proton energy in Mev, which holds in the center-of-mass coordinate system. The tracks were counted in various areas, depending on the track density, then multiplied by an appropriate factor so that they would all correspond to a "standard" area of 0.140-in. length by 4-squares width (0.176 mm) in the counting reticle. Calculating this solid angle and putting it in the scattering formula, along with the beryllium-foil data, the following working formula is obtained:

$$N_R=\frac{184.}{\beta E^2},$$

where N_R is the number of tracks in the "standard" counting area.

The correction of the observed angles and yield to C.M. coordinates was made on the assumption that the observed particles were elastically scattered protons, for which $\alpha=\frac{1}{9}$ (independently of E_p, since $Q=0$).

The resulting yield data was treated in several ways to see what analysis would be most suitable. The ratio of the observed yield to the calculated Rutherford scattering was plotted against $\cos\theta_c$ for each plate. This is shown in Fig. 6. These curves show that the deviation from Rutherford scattering becomes very marked at large angles, especially at the higher energies used.

The data is also plotted as total yield minus Rutherford scattering in Fig. 7. Since the ratio to Rutherford scattering is large at large angles, the total yield at the large angles becomes more nearly equal to the additional yield as interference effects become small, if it is assumed that the additional yield is due to resonance scattering of protons. The two wave functions will give interference terms which will be strong where the two primary intensities are of equal magnitude, but the total yield will be not much different from the larger, when one is much stronger than the other. For this reason the yield at large angles minus Rutherford scattering ought to be a reasonable estimate of the additional effect caused either by resonance scattering or by another reaction. The fact that these curves rise sharply at small angles indicates the probability that the increase is due to interference terms between resonance yield of protons and the Rutherford scattering, as the yield of alphas or deuterons would not show any interference effect.

Figure 5 gives excitation curves of the resonance scattering at various angles. The points are taken from the smoothed curves of Fig. 6. They show two maxima which appear to correspond to the two γ-ray-emitting levels, although considerably broadened. Figure 5 also shows the γ-ray yield from a beryllium foil of the same thickness. The very considerable broadening of the reso-

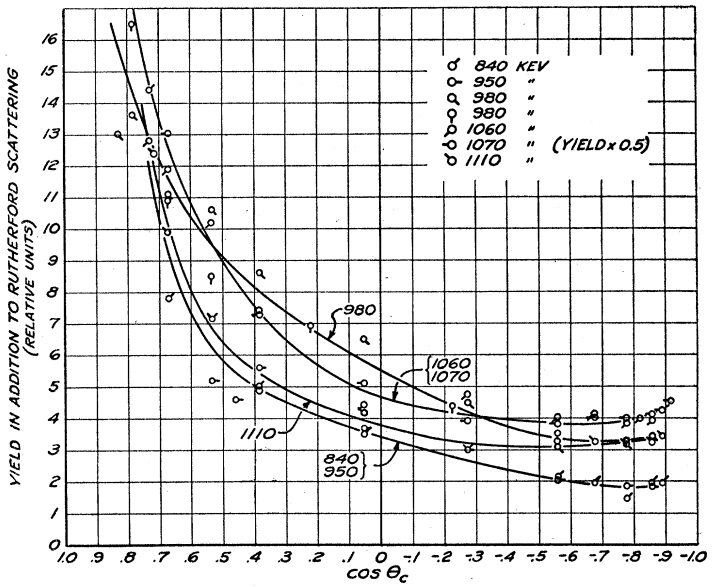

FIG. 7. Total yield after subtracting Rutherford scattering at various proton energies.

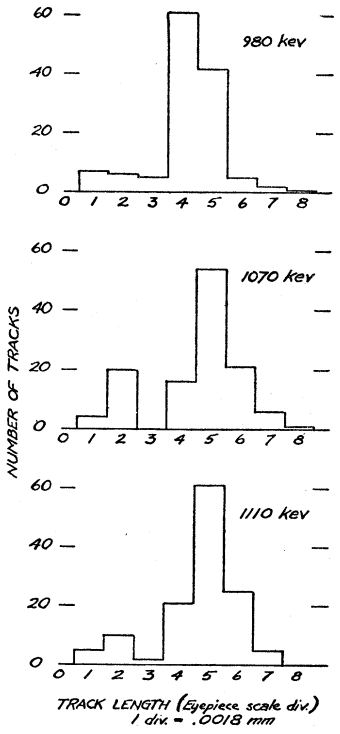

FIG. 8. Range distribution curves. Maximum is at correct range in emulsion for scattered protons; group at ~2 div. range is approximately range of alphas from $Be^9(p, \alpha)Li^6$. Deuterons from $Be^9(p, d)Be^8$ are not distinguishable from protons.

nances for scattering, especially at the low energy side, cannot be accounted for solely by interference with Rutherford scattering, which would tend to shift the resonance toward higher energy, but appears to require additional scattering by adjacent levels. Some variation of the energy of the maximum with the angle of observation can be explained by interference effects, which will vary with angle. The results must be considered to be of a preliminary nature.

It is difficult to correlate the width of the broad γ-ray resonance with the large ratio of total yield to Rutherford scattering observed at large angles, since the width of 100 kev seems to require s-wave protons for γ-ray production, yet for s-wave protons, using Bethe's formula for the ratio of total yield to Rutherford scattering,[30] the maximum scattering ratio at 180° is about 7. If we assume that the deuteron yield is of the same order of magnitude as the alpha-yield which may be about 20 percent of the total, as shown in Fig. 8, then in the backward direction they would make up about half the total yield. In that case the ratio of the remaining yield, which would be the resonance-scattered protons, to the Rutherford scattering would be brought down to about 6, but the theoretical ratio would be somewhat reduced from 7 by the increased total width, so that this is not a satisfactory explanation. Another possibility is that we are dealing with more than one resonance in the emission of heavy particles, or that there is a strong background in addition to the resonance, which could change the critical quantities sufficiently to account for this effect with resonance scattering of s-wave protons. It may also be that the broad γ-ray resonance is due to p-wave protons, and that it is the large width which needs to be explained.

The author is grateful to Professors C. C. Lauritsen, T. Lauritsen, R. F. Christy, and W. A. Fowler for their aid and advice in this work.

This work was carried out under contract of the laboratory with the Office of Naval Research, and under a fellowship grant to the author from the National Research Council.

[30] H. A. Bethe, Rev. Mod. Phys. 9, 176 (1937), formula 625.